

# UC Riverside

## UC Riverside Previously Published Works

### Title

Effect of hydrogen addition on criteria and greenhouse gas emissions for a marine diesel engine

### Permalink

<https://escholarship.org/uc/item/4zi730vc>

### Journal

International Journal of Hydrogen Energy, 39(21)

### ISSN

0360-3199

### Authors

Pan, Hansheng  
Pournazeri, Sam  
Princevac, Marko  
et al.

### Publication Date

2014-07-01

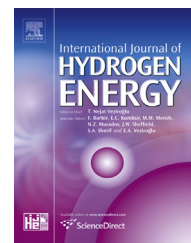
### DOI

10.1016/j.ijhydene.2014.05.010

Peer reviewed

Available online at [www.sciencedirect.com](http://www.sciencedirect.com)

ScienceDirect

journal homepage: [www.elsevier.com/locate/ije](http://www.elsevier.com/locate/ije)

## Effect of hydrogen addition on criteria and greenhouse gas emissions for a marine diesel engine

Hansheng Pan<sup>a</sup>, Sam Pournazeri<sup>a</sup>, Marko Princevac<sup>a,\*</sup>, J. Wayne Miller<sup>b,c</sup>, Shankar Mahalingam<sup>a,1</sup>, M. Yusuf Khan<sup>b,c</sup>, Varalakshmi Jayaram<sup>b,2</sup>, William A. Welch<sup>c</sup>

<sup>a</sup> Department of Mechanical Engineering, Bourns College of Engineering, University of California, Riverside, CA 92521, USA

<sup>b</sup> Department of Chemical and Environmental Engineering, Bourns College of Engineering, University of California, Riverside, CA 92521, USA

<sup>c</sup> Center for Environmental Research and Technology, College of Engineering, University of California, Riverside, CA 92521, USA

### ARTICLE INFO

#### Article history:

Received 15 January 2014

Received in revised form

9 April 2014

Accepted 2 May 2014

Available online 9 June 2014

#### Keywords:

Dual fuel internal combustion engine

Hydrogen addition

Diesel engine

PM

NO<sub>x</sub>

Fuel consumption

### ABSTRACT

Hydrogen remains an attractive alternative fuel to petroleum and a number of investigators claim that adding hydrogen to the air intake manifold of a diesel engine will reduce criteria emissions and diesel fuel consumption. Such claims are appealing when trying to simultaneously reduce petroleum consumption, greenhouse gases and criteria pollutants. The goal of this research was to measure the change in criteria emissions (CO, NO<sub>x</sub>, and PM<sub>2.5</sub>) and greenhouse gases such as carbon dioxide (CO<sub>2</sub>), using standard test methods for a wide range of hydrogen addition rates. A two-stroke Detroit Diesel Corporation 12V-71TI marine diesel engine was mounted on an engine dynamometer and tested at three out of the four loads specified in the ISO 8178-4 E3 emission test cycle and at idle. The engine operated on CARB ultra-low sulfur #2 diesel with hydrogen added at flow rates of 0, 22 and 220 SLPM.

As compared with the base case without hydrogen, measurements showed that hydrogen injection at 22 and 220 SLPM had negligible influence on the overall carbon dioxide specific emission, EF<sub>CO<sub>2</sub></sub>. However, in examining data at each load the data revealed that at idle EF<sub>CO<sub>2</sub></sub> was reduced by 21% at 22 SLPM (6.9% of the added fuel energy was from hydrogen) and 37.3% at 220 SLPM (103.1% of the added fuel energy was from hydrogen). At all other loads, the influence of added hydrogen was insignificant. Specific emissions for nitrogen oxides, EF<sub>NO<sub>x</sub></sub>, and fine particulate matters, EF<sub>PM<sub>2.5</sub></sub>, showed a trade-off relationship at idle. At idle, EF<sub>NO<sub>x</sub></sub> was reduced by 28% and 41% with increasing hydrogen flow rates, whilst EF<sub>PM<sub>2.5</sub></sub> increased by 41% and 86% respectively. For other engine loads, EF<sub>NO<sub>x</sub></sub> and EF<sub>PM<sub>2.5</sub></sub> did not change significantly with varying hydrogen flow rates. One of the main reasons for the greater impact of hydrogen at idle is that the contribution of hydrogen to

\* Corresponding author. Tel.: +1 951 827 2445; fax: +1 951 827 2899.

E-mail address: [marko@engr.ucr.edu](mailto:marko@engr.ucr.edu) (M. Princevac).

<sup>1</sup> Present address: Department of Mechanical and Aerospace Engineering, College of Engineering, The University of Alabama in Huntsville, AL 35899, USA.

<sup>2</sup> Present address: ENVIRON, 18100 Von Karman Avenue, Suite 600 Irvine, CA 92612, USA.

<http://dx.doi.org/10.1016/j.ijhydene.2014.05.010>

0360-3199/Copyright © 2014, Hydrogen Energy Publications, LLC. Published by Elsevier Ltd. All rights reserved.

the total fuel energy is much higher at idle as compared to the other loads. The final examination in this paper was the system energy balance when hydrogen is produced by an on-board electrolysis unit. An analysis at 75% engine load showed that hydrogen production increased the overall equivalent fuel consumption by 2.6% at 22 SLPM and 17.7% at 220 SLPM.

Copyright © 2014, Hydrogen Energy Publications, LLC. Published by Elsevier Ltd. All rights reserved.

Nomenclature			
A/F ratio	air/fuel ratio	kW	kilowatt
BSFC	brake specific fuel consumption, g/kW-h	LHV	lower heating value, kJ/kmol
BSU	Bosch Smoke Unit, BSU	min	minutes
CARB	California Air Resources Board	NO <sub>x</sub>	oxides of nitrogen
CO	carbon monoxide	OC	organic carbon
CO <sub>2</sub>	carbon dioxide	PM	particulate matter
DAF	dilution air filter	PTFE	polytetrafluoroethylene or teflon filter
DT	dilution tunnel	ppm	parts per million
EF	specific emission, g/kW-h	RGA	residual gas analyzer
EGA	exhaust gas analyzer	RPM	revolutions per minute
EPA	Environmental Protection Agency	SLPM	standard liter per minute
g/kW-h	grams per kilowatt-hour	TDI	turbocharged direct injection
ICEs	internal combustion engines	THC	total hydrocarbons
ISO	International Organization for Standardization	UCR	University of California, Riverside
kg/m <sup>3</sup>	kilograms per cubic-meter	VN	Venturi
		v%	volume %

## Introduction

Hydrogen is considered as an alternative source of energy for a sustainable system and improved air quality. Hydrogen has some unique features compared to hydrocarbons, such as high mass and thermal diffusivity, wide range of flammability limits, low minimum ignition energy, and high stoichiometric air-to-fuel ratio. With these properties, hydrogen is an ideal fuel to combine with other fuels or solely used to potentially improve combustion and emission response [1]. Rakopoulos et al. [2] pointed out that hydrogen's potential for increased second-law efficiency is possibly one of the most significant advantages. The application of hydrogen injection control technology in internal combustion engines (ICEs) was proposed in the 1970's. Since then, there have been numerous hydrogen engine-powered vehicles ranging from two-wheelers to passenger cars, pickup trucks and buses that have been designed, built and tested. Many studies have implemented the use of hydrogen as a fuel in spark ignition (SI) engines [3]. However, these studies showed that using hydrogen in SI engines would lead to substantial drop in power output as well as the occurrence of backfire and knocking problems at high loads due to the spontaneous combustion of hydrogen [4]. Thus, the use of hydrogen in SI engines is limited to a certain range of operating conditions [5].

Due to the relatively high self-ignition temperature of hydrogen and the inability of compression to reach that limit, previous studies looked into technologies that supplied hydrogen into diesel fuel ICEs (dual fuel mode) with the purpose of reducing criteria air pollutants and greenhouse gases simultaneously. Varde and Frame [6] carried out an experimental study on a single cylinder, four-stroke direct injection diesel engine. It was reported that at full load, the brake thermal efficiency increased from 30.5% to 33.7% with approximately 12.5% of the energy supplied by hydrogen. The improved thermal efficiency was attributed to the increased combustion efficiency. Bika et al. [7] tested a 1999 Volkswagen 4 cylinder, 1.9 L TDI diesel engine. Results showed that when 10% and 40% of the energy were supplied by hydrogen, PM emissions reduced by 10% and 50% respectively. Kumar et al. [8] investigated the addition of hydrogen into a vegetable oil fueled compression ignition engine. Results indicated that the brake thermal efficiency increased from 27.3% to a maximum of 29.3% at 7% of hydrogen mass share at maximum power output. Smoke was reduced by 16% of Bosch Smoke Unit (BSU) at the best efficiency point. HC and CO emissions decreased by 23% and 35% by volume respectively at maximum power output. NO level increased by 16% at full output due to higher combustion temperature. Tsolakis et al. [9] conducted experiments that showed that diesel engine exhaust particulate emissions can be reduced by the use of hydrogen-rich gas that is produced by the catalytic reaction of diesel fuel and exhaust gas. There is also evidence

that supplement of H<sub>2</sub> to light-duty diesel engine leads to a reduction in PM emissions when the engine is operated at low, and medium to high load [10–12]. Tomita et al. [10] investigated a four-stroke diesel engine with a single cylinder. Their experiments showed that smoke was decreased to almost zero when hydrogen was mixed with inlet air. HC, CO and CO<sub>2</sub> emissions decreased with increasing fraction of hydrogen. Brake thermal efficiency was slightly lower than in ordinary diesel combustion. NO<sub>x</sub> emissions increased or decreased under various conditions. Tomita et al. [10] explained that NO<sub>x</sub> emissions decreased because of lean premixed combustion that is devoid of a region of high temperature of burned gas such as seen in ordinary diesel operations. He observed that such a situation occurred when the injection timing of diesel into the cylinder is extremely advanced.

Recently, some commercial units produce a mixture of hydrogen and oxygen (H<sub>2</sub>/O<sub>2</sub>) on-board by water electrolysis [13]. Bari et al. [14] investigated the impacts of adding H<sub>2</sub>/O<sub>2</sub> mixture on the performance parameters of a diesel engine coupled to a generator producing electricity. The engine was tested with the addition of varying amount of H<sub>2</sub>/O<sub>2</sub> mixture (1–6%) under three different load levels of 19, 22 and 28 kW. The H<sub>2</sub>/O<sub>2</sub> mixture was generated using 24 V external power supply and the power needed to produce the H<sub>2</sub>/O<sub>2</sub> mixture is included in the input energy of the engine. Their experimental results showed that adding a 6.1% H<sub>2</sub>/O<sub>2</sub> mixture resulted in a 2.6% increase in brake thermal efficiency at 19 kW, 2.9% at 22 kW, and 1.6% at 28 kW. However, beyond 5% addition, no significant effect was found in enhancing the engine performance.

To date, very little research on supplementing H<sub>2</sub> to a modern heavy-duty diesel engine has been conducted especially for off-road applications. In many coastal areas, low-speed marine diesel engines are primary sources of PM and NO<sub>x</sub> [15]. Hence, the objective of this study was to evaluate and assess the impact of hydrogen injection control technology on marine or related diesel engines.

For this study, a two-stroke MTU/Detroit diesel engine was tested on an engine dynamometer at load points specified for engine certification and at idle since that is a common operating mode. Each load point was tested in duplicate for three hydrogen flow rates: 0, 22 and 220 SLPM. Hydrogen flow rate of 0 SLPM represents the baseline condition, and a flow rate of 22 SLPM is comparable to existing commercial products. A hydrogen flow rate of 220 SLPM is ten times the recommended commercial levels and was selected to ensure that sufficient hydrogen was available to produce measurable effects, while maintaining the hydrogen–air mixture composition below the lower flammability limit.

## Experimental setup

### Engine and fuel description

A well-maintained MTU/Detroit Diesel 12V-71TI marine diesel engine was used as a test engine. The specifications for the engine are summarized in Table 1. Ultra-low sulfur, CARB No. 2 diesel and cylinder hydrogen were used for all tests. The engine was mounted on a Taylor heavy-duty, water-brake engine dynamometer.

**Table 1 – Engine properties.**

Basic engine	12V-71TI
Description	Turbocharged, Intercooled Pleasure craft engine
Engine type	Two stroke
Number of cylinders	12
Bore and stroke	114.3 mm × 127 mm
Displacement-two cycle (Every downstroke a powerstroke)	13,961 cm <sup>3</sup>
Rated brake kilowatts	503@2300 RPM
Rated shaft kilowatts	485@ 2300 RPM
Compression ratio	17 to 1
Approx. net weight (dry) with standard equipment	2359 kg

### Test cycles

A standard test cycle was selected to measure the effects of added hydrogen. Two duty cycles are used to certify marine engines. One cycle assumes engines operate on a fixed-pitch propeller curve (E3), and the other is for propulsion engines that operate at a constant speed (E2). Fixed-pitch propellers are used in most commercial vessels such as tugs, draggers, fishing vessels, and trawlers. In this study, we selected the ISO 8178-4 E3, four-mode test cycle [16] shown in Table 2 together with 4% load to represent idle. The first step involved mounting the engine securely on a water-brake dynamometer and measuring the engine map for the full load range. Selected ISO 8178-E3 four-mode test cycles together with measured test conditions are shown in Fig. 1.

### Specialized hydrogen injection system

Hydrogen was supplied from a high-pressure six-pack of cylinders, each at 150 bars to an outlet pressure of 1 bar using a hydrogen pressure regulator. A fine control valve was used to adjust the flow rate of hydrogen through a mass flow meter (Smart-Trak 2 Series 100, Sierra Instruments) with a digital readout of flow. A flame arrestor was installed prior to where the hydrogen supply was split into two injection ports, to improve mixing of hydrogen with air in the intake.

### Sampling and analysis

A schematic of hydrogen injection system and emissions sampling is provided in Fig. 2. During the test, the

**Table 2 – Test modes and weighting factors for marine applications (ISO-8178-4 E3).**

Mode	Power		Speed		Weighting factors
	kW	%	RPM	%	
ISO-8178-4 E3 cycle	384	100	2053	100	0.2
	288	75	1868	91	0.5
	192	50	1642	80	0.15
	96	25	1293	63	0.15
Idle	15	4	657	32	0

hydrogen–air mixture and exhaust are collected into Tedlar bags and later analyzed by Residual Gas Analyzer (RGA). RGA calculated average partial pressure of each gas in the mixture over the duration time of scans, and then calculated volume percentage of each gas in air mixture.

The sampling and analysis of gases and particulate matter (PM) followed the ISO 8178-1 standards [17]. The concentrations of CO<sub>2</sub> or NO<sub>x</sub> were measured in the raw exhaust gas and in the dilution tunnel using the Horiba PG-250 exhaust gas analyzer (EGA), to determine the dilution ratio. The EGA used in this study utilizes an electronic cooler for removal of water vapor to minimize losses of acidic gases such as NO<sub>x</sub> due to their solubility in the water condensate (dry based measurement). According to Tier 4 Standards for marine Diesel engines [18], THC emissions are less than 10% of the NO<sub>x</sub> emissions. Therefore, as part of the criteria pollutant analysis performed in this paper, we only focused on NO<sub>x</sub> and PM emissions which play a significant role in the near port air quality.

The test was conducted from high load to low engine load as specified in the ISO standard and from low to high hydrogen flow rate at each constant engine load. Duplicate measurements were made at each load and data showed that between each change in engine load or fuel it takes about 5 min for the system to restore its steady state conditions.

#### Calculation of the mass emission rates

Mass emission rates are determined from the measured concentrations and the mass flow rates in the exhaust. For this study, we measured the diesel fuel flow into the engine and used the carbon balance method as specified in ISO 8178-1 to calculate the exhaust flow rate. As previously investigated by our team [19], the carbon balance method has a very good agreement with the method using the engine as an air pump. The carbon balance method assumes a control volume system and that carbon entering in the fuel leaves as CO<sub>2</sub>. The exhaust volumetric flow rate in SCFM was calculated as:

$$EFR \text{ I[SCFM]} = \frac{C_F \times 24.47 \times F_c [\text{lb}/\text{min}] \times 0.4536 \times 0.03531 \times 0.001}{12 \times (RC_{CO_2} [\%] - 0.03 [\%])} \quad (1)$$

where  $C_F = 0.87$  is carbon content of fuel, 24.47 is specific mole based volume of CO<sub>2</sub> in L/mol,  $F_c$  is fuel consumption in lb/min, 0.4536 is the conversion between lb and kg, 0.03531 is the conversion between ft<sup>3</sup> and liter, 0.001 is the conversion between g and kg, 12 is the molecular weight of carbon in g/mol,  $RC_{CO_2}$  is the raw concentration of CO<sub>2</sub> measured by EGA (dry based measurements,  $g_{CO_2}/g_{air}$ ), and 0.03 is the background concentration of CO<sub>2</sub>.

To convert the measured CO<sub>2</sub> concentration from % to kg/h, equation (2) was used:

$$CO_2 [\text{kg}/\text{h}] = \frac{RC_{CO_2} [\%] \times 0.01 \times MW_{CO_2} [\text{kg}/\text{kmol}] \times EFR \text{ I[SCFM]} \times 28.3 [\text{L}/\text{ft}^3] \times 60 [\text{min}/\text{h}]}{1000 \times 24.47 [\text{L}/\text{mol}]} \quad (2)$$

where 24.47 L/mol is the specific mole based volume of CO<sub>2</sub>.

The CO<sub>2</sub> specific emission is calculated as:

$$EF_{CO_2} [\text{g}/\text{kW}\cdot\text{h}] = \frac{CO_2 [\text{kg}/\text{h}] \times 1000}{\text{power} [\text{kW}]} \quad (3)$$

Since PM was collected in the dilution tunnel, the impact of dilution ratio is reflected as:

$$PM [\text{g}/\text{h}] = \frac{PM [\text{mg}/\text{filter}] \times 0.001 [\text{g}/\text{mg}] \times \text{Dilution Ratio}}{\text{Flow Rate}_{\text{filter}} [\text{L}/\text{min}] \times 0.001 [\text{m}^3/\text{L}] \times \text{Time} [\text{min}]} \times \text{Flow Rate}_{\text{exhaust}} [\text{m}^3/\text{h}] \quad (4)$$

$$EF_{PM} [\text{g}/\text{kW}\cdot\text{h}] = \frac{PM [\text{g}/\text{h}]}{\text{power} [\text{kW}]} \quad (5)$$

#### Data analysis: calculation of overall emissions factors

Emissions were measured from idle to 75% load and specific emissions were calculated for each mode. Since the 100% load for the tested engine exceeded the limit of our dynamometer setup, the emissions data was extrapolated to estimate the specific emission at 100% load. Such extrapolation may induce some uncertainties, as the response of diesel engine at full load can be significantly different compared to low and medium load. However, this extrapolation allowed us to calculate the overall specific emissions of NO<sub>x</sub>, CO<sub>2</sub>, and PM as,

$$A_{WM} = \frac{\sum_{i=1}^n (g_i \times WF_i)}{\sum_{i=1}^n P_i \times WF_i} \quad (6)$$

where  $A_{WM}$  is weighted mass emission level (HC, CO, CO<sub>2</sub>, PM, or NO<sub>x</sub>) in g/kW-h,  $g_i$  is emission in g/h,  $P_i$  is power measured during each mode (includes auxiliary loads), and  $WF_i$  is effective weighting factor for an ISO 8178-4 E3 cycle (Table 2). Note that 80% of the weighting comes from the measured data and only 20% comes from the value estimated at 100% load, which minimizes the uncertainties involved with the above-mentioned extrapolation.

## Results and discussion

The emissions measured during hydrogen injection are compared with the baseline. For reference, the results were also compared with EPA Tier 2 certification standards. The percentage of total fuel energy provided by H<sub>2</sub> and its volumetric addition to the intake air (in percent of total intake volume) for each load are listed in Table 3. Data were taken in duplicate and average values for each mode are presented in the following sections.

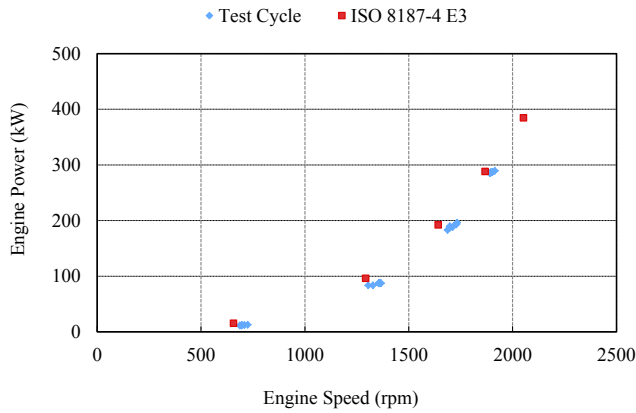


Fig. 1 – Test engine map.

Gaseous emissions

Emissions of gases, CO, CO<sub>2</sub> and NO<sub>x</sub> were measured over the modes identified in the ISO 8178-4 E3 cycle. Both CO<sub>2</sub> and NO<sub>x</sub> emissions were analyzed in order to make sure that the repeatability of the data was within expected limits.

During testing, CO<sub>2</sub> emissions increased linearly with load as expected with coefficients of determination R<sup>2</sup> of 0.99. This finding is consistent with the linear relationship of the amount of fuel consumed and the output shaft power in the specified range. NO<sub>x</sub> emissions also increased linearly with load with R<sup>2</sup> in the range from 0.96 to 0.98. Table 4 lists the parameters as well as the correlation coefficients of linear fits between emissions and engine loads. These parameters were used to estimate emissions at 100% load. The variation of EF<sub>CO<sub>2</sub></sub> (g/kW-h) with hydrogen addition at different engine loads is shown in Fig. 3. At idle, the reductions in EF<sub>CO<sub>2</sub></sub> were 21% and 37% when energy added by H<sub>2</sub> is 6.9% and 103.1% (i.e. the energy added by hydrogen is 1.03 times that of diesel at 220 SLPM hydrogen injection) respectively. At 50% load, EF<sub>CO<sub>2</sub></sub>

Table 3 – The percentage of energy and volumetric addition of hydrogen to the intake air.

Load	Commercial value (22 SLPM)		High level (220 SLPM)	
	Energy % <sup>a</sup>	Volume %	Energy % <sup>a</sup>	Volume %
Idle	6.9	0.23	103.1	2.83
25%	1.6	0.11	15.0	1.08
50%	0.7	0.07	8.2	0.77
75%	0.5	0.05	5.2	0.58

<sup>a</sup> Percentage of energy added by hydrogen with respect to the energy added by diesel fuel (i.e. During idle condition, the 103% added energy means that energy added by hydrogen is almost 1.03 times that of diesel at 220 SLPM hydrogen injection.).

reduced by 7% and 12% when energy added by H<sub>2</sub> is 0.7% and 8.2%. At high load (75% load), the changes in EF<sub>CO<sub>2</sub></sub> were within the measurement errors as energy added by H<sub>2</sub> were 0.5% and 5.2%. The change of overall weighted specific emissions was within measurement errors when H<sub>2</sub> flow rate was 22 SLPM. It reduced 3% when H<sub>2</sub> flow rate was 220 SLPM.

Hydrogen engines can run on A/F ratios ranging from 34:1 (stoichiometric) to 180:1 [20]. The critical equivalence ratio ( $\phi$ ) for NO formation in high-temperature/high-pressure burned gases is close to unity for both a gasoline engine and a diesel engine. Equivalence ratio ( $\phi$ ) is defined as the stoichiometric A/F ratio divided by the actual A/F ratio [21]. Our results in Fig. 4 showed an increase of EF<sub>NO<sub>x</sub></sub> relative to  $\phi$  from idle to 50% when hydrogen was injected into a diesel engine.

As explained by Frassoldati et al. [22], the primary sources of NO<sub>x</sub> formation from hydrocarbon fuel, without the nitrogen content, are thermal and prompt [23] processes. In thermal process, the high temperature of the combustion oxidizes the diatomic nitrogen, thereby creating NO through the Zeldovich mechanism. In the prompt process, the reaction of nitrogen with radicals such as C, CH, and CH<sub>2</sub> forms nitrogen species: NH, HCN, H<sub>2</sub>CN and CN. These species can further oxidize and form NO.

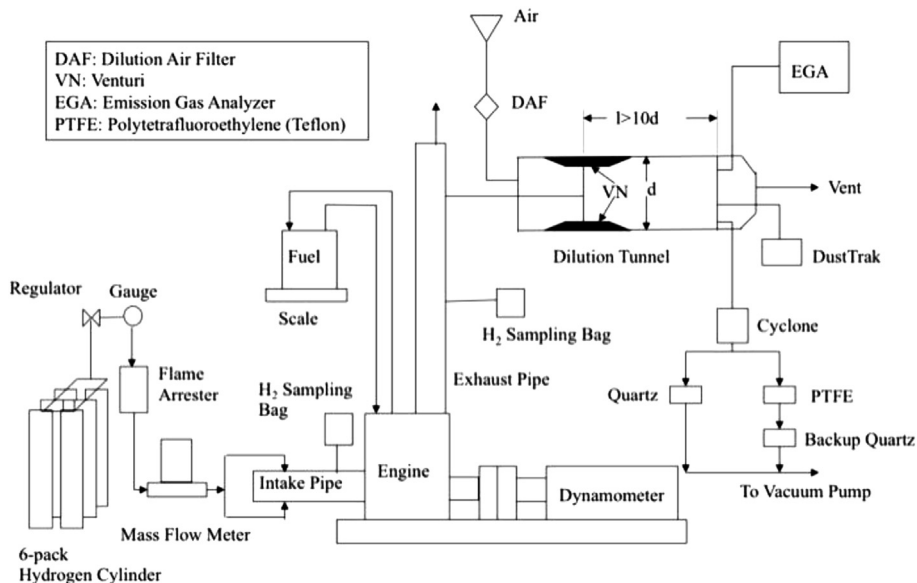


Fig. 2 – Flow diagram of the hydrogen injection system and the sampling system.

**Table 4 – Linear fittings between emissions and engine loads.**

Emissions	Baseline (0 SLPM)		Commercial value (22 SLPM)		High level (220 SLPM)	
	a	R <sup>2</sup>	a	R <sup>2</sup>	a	R <sup>2</sup>
CO <sub>2</sub>	0.697	0.99	0.689	0.99	0.670	0.99
CO	$1.27 \times 10^{-3}$	0.57	$1.34 \times 10^{-3}$	0.75	$1.38 \times 10^{-3}$	0.79
NO <sub>x</sub>	$1.09 \times 10^{-2}$	0.98	$1.08 \times 10^{-2}$	0.97	$1.03 \times 10^{-2}$	0.96
PM	0.371	0.90	0.338	0.98	0.328	0.92

Notes: a – parameters in linear fittings; R<sup>2</sup> – correlation coefficient.

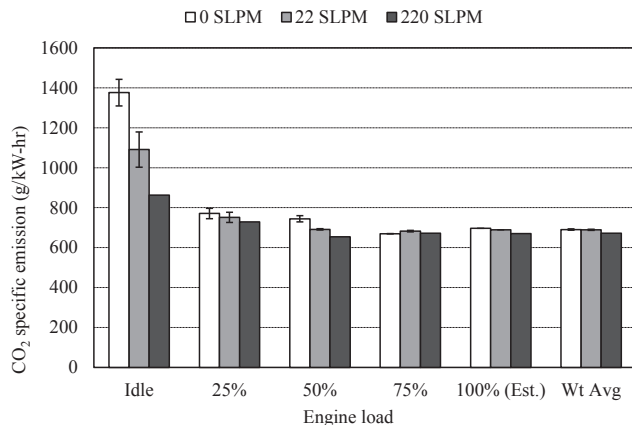
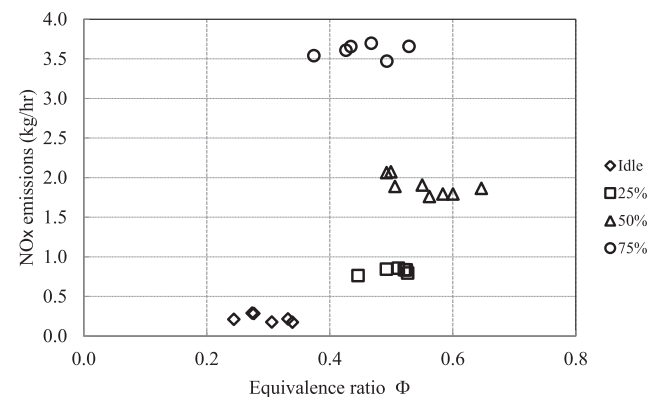
As discussed by Heywood [21], for a compression ignition engine, the peak NO concentrations occurs when burned gas temperatures are at a maximum, which is between the start of combustion and shortly after the occurrence of peak cylinder pressure. Therefore, burned gas temperatures decrease due to cylinder gas expansion and mixing of high-temperature gas with air [24]. The cooler burned gas freezes the NO chemistry resulting in a reduction in NO concentrations. Heywood [21] also investigated the ratio of local NO concentration to exhaust NO concentration. It was found that almost all of the NO formation occurs within the 20° crank angle following the start of combustion [17]. The retarded injection timing could cause the retarded combustion process at which it reduces the peak temperatures and subsequently lowers the NO concentrations.

Fig. 5 shows the variation of EF<sub>NO<sub>x</sub></sub> with varying H<sub>2</sub> addition at each load. At 75% load, the variation of EF<sub>NO<sub>x</sub></sub> were within the measurement errors when 0.5% and 5.2% of total energy was added by H<sub>2</sub>. Although, addition of hydrogen tends to suppress prompt NO<sub>x</sub> formation, it increases the flame temperature and extends the flammability limits of the mixture [22]. This will enhance thermal NO<sub>x</sub> formation and cause an increase in the NO<sub>x</sub> emission rate for stoichiometric equivalence ratio of  $\phi \approx 1$ . The effect of hydrogen as well as flame temperature on thermal NO<sub>x</sub> formation is extensively discussed in the literature [22,25,26]. However, at lower load, under leaner conditions ( $\phi < 1$ ), results show a decrease in NO<sub>x</sub> emissions with injection of H<sub>2</sub>. A study by White et al. [27] reported that the addition of hydrogen allows a more complete combustion under ultra-lean ( $\phi < 0.5$ ) conditions. This results in a significant decrease in combustion temperature and thus suppression of

thermal NO<sub>x</sub> [28]. For example, at 50% load, EF<sub>NO<sub>x</sub></sub> reduced 10% and 15% when 0.7% and 8.2% energy were added by H<sub>2</sub>; at idle EF<sub>NO<sub>x</sub></sub> reduced 28% and 41% when 6.9% and 103.1% of total energy were added by H<sub>2</sub>. The overall specific emissions were unchanged with H<sub>2</sub> flow rate of 22 SLPM while they were reduced by 4% with H<sub>2</sub> flow rate of 220 SLPM.

Rortveit et al. [25] investigated the impact of diluents on NO<sub>x</sub> formation in hydrogen flames. Although in his experiments, the diluents were mainly N<sub>2</sub>, He, and CO<sub>2</sub>, he showed that significant reduction in NO<sub>x</sub> emission occurs as a result of reduction in flame temperature. Further, Frassoldati et al. [22] showed that at high dilution, the path to thermal NO<sub>x</sub> is nearly eliminated and NO<sub>x</sub> will be generated only through the NNH and nitrous reactions [29]. Here in this study we hypothesized that unburned H<sub>2</sub>, which survived the main combustion process, acts as a diluent and reduces flame temperatures at low loads rather than increasing it through the hydrogen combustion. Note that the heat capacity of H<sub>2</sub> per mole at the temperatures relevant to diesel combustion is a little higher than that of N<sub>2</sub>.

Previous studies [30,31] reported that the H<sub>2</sub> present outside of the diesel spray plume might survive the main combustion process due to the lack of a propagating flame. The survived hydrogen will exit diesel engine as unburned fuel. Furthermore, one of the essential processes in two-stroke engines is cylinder scavenging where about 25% of the intake mixture flow is used to scavenge the exhaust gas. The hydrogen content of the intake air will be added to the unburned hydrogen from the combustion. In this study, RGA was used to measure hydrogen volume percentage in both intake mixture and exhaust to analyze any unburned hydrogen. RGA measured H<sub>2</sub> were corrected by a CO<sub>2</sub> correlation factor, which

**Fig. 3 – Modal and overall emission factors for CO<sub>2</sub>.****Fig. 4 – NO<sub>x</sub> emissions vs. equivalence ratio.**

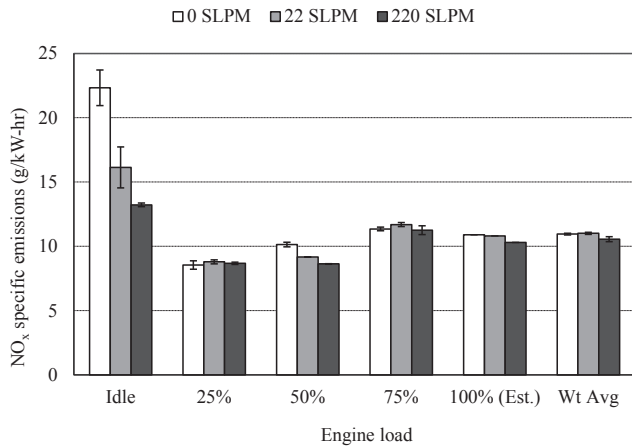


Fig. 5 – Modal and overall emission factors for NO<sub>x</sub>.

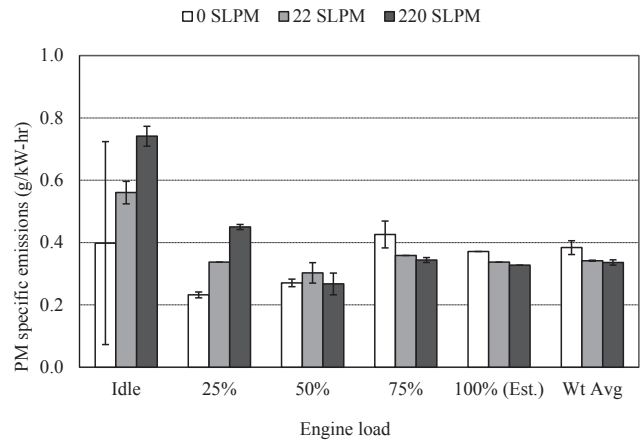


Fig. 7 – Modal and overall emission factors for weighted PM.

is the ratio of EGA CO<sub>2</sub> to RGA CO<sub>2</sub>. In most cases H<sub>2</sub> in the exhaust was at the noise level. Although, this is an interesting result, its correctness needs to be further investigated.

The variation of EF<sub>CO</sub> with hydrogen addition is shown in Fig. 6. At 75% load, EF<sub>CO</sub> increased 10% and 14% when 0.5% and 5.2% of total energy were added by H<sub>2</sub>. At idle, CO emissions decreased 22% and 47% when 6.9% and 103.1% of total energy were added by H<sub>2</sub>. The overall weighted EF<sub>CO</sub> increased 7% and 11% with H<sub>2</sub> flow rates of 22 and 220 SLPM.

Particulate matter (PM<sub>2.5</sub>) emissions

PM<sub>2.5</sub> mass was measured by several independent methods to assure the quality of the data. One method, which is the federal reference method, measures PM<sub>2.5</sub> mass collected on a Teflon filter. A second method collects soot on a quartz filter and the filter is subsequently analyzed for elemental and organic carbon mass. Real-time particulate matter concentrations were measured by TSI DustTrak 8520 (TSI, Inc.). A linear correlation was observed between DustTrak and mass collected on Teflon filter with R<sup>2</sup> ~0.78. As expected the DustTrak PM values are lower by a factor of 2–3 [32].

The correlation coefficient of a linear fit between PM emission rates and loads are greater than 0.90 as seen in Table 4. Compared to EF<sub>NO<sub>x</sub></sub>, EF<sub>PM</sub> shows opposite trend at idle and 75% as evident from Fig. 7. At 75%, EF<sub>PM</sub> decreased 16% and 19% when 0.5% and 5.2% of total energy were added by H<sub>2</sub>. As discussed earlier, hydrogen addition increases flame temperature at high load which in turn improves the combustion of hydrocarbon and inhibits PM formation. Considering the lean combustion at idle condition, it is hypothesized that hydrogen addition manifested as diluents that reduced the burned gas temperature and increased the amount of unburned hydrocarbons. The results in Fig. 7 show that at idle, EF<sub>PM</sub> increased 41% and 86% when 6.9% and 103.1% of total energy were added by H<sub>2</sub> respectively. The error at idle with no H<sub>2</sub> addition (0 SLPM) is about 75% suggesting that further research is required to explain the trend of EF<sub>PM</sub> at idle. Since idle is not included in weighted specific emissions, this large uncertainty does not affect the overall results of the present study. At 25% load, EF<sub>PM</sub> also increased with H<sub>2</sub> injection. The weighted specific emissions with H<sub>2</sub> flow of 22 and 220 SLPM

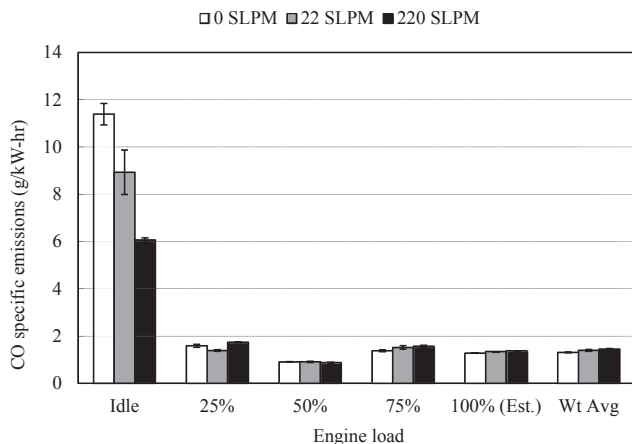


Fig. 6 – Modal and overall emission factors for CO.

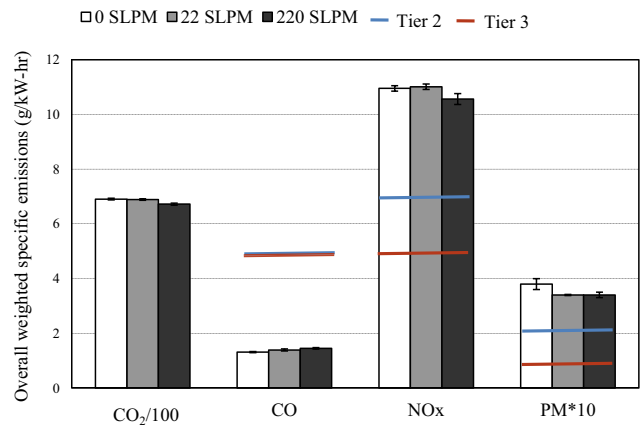


Fig. 8 – Overall weighted average emission factors for gases and PM<sub>2.5</sub> with hydrogen flow rates of 0, 22 and 220 SLPM under the test cycle of E3. Note that Tier 2 and Tier 3 standards on the NO<sub>x</sub> bars represent NO<sub>x</sub> + THC.



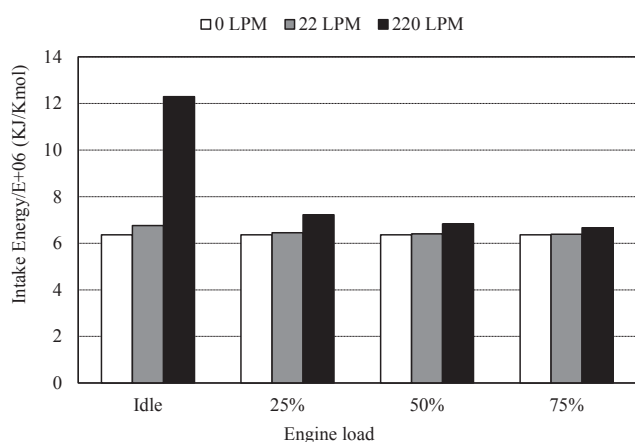


Fig. 9 – Intake energy vs. loads.

decreased by 11% over the baseline condition. This is mainly due to the reduction of PM specific emission at 75% load which has the highest weight (weighting factor of 0.5) in the overall weighted specific emission calculation.

#### Overall weighted specific emissions under E3 cycle

The overall weighted specific emissions are calculated based on equation (6) presented in Section [Data analysis: calculation of overall emissions factors](#). Fig. 8 shows the overall weighted specific emission for gases and PM along with the certification values for Tier 2 and Tier 3 engines. With H<sub>2</sub> flow rates of 22 SLPM and 220 SLPM, NO<sub>x</sub> weighted specific emissions increased by 1% and reduced by 4%. PM weighted specific emissions reduced by 11% for both H<sub>2</sub> flow rates.

#### Intake energy

Since hydrogen was supplied to the intake air, the overall intake energy was increased. Added energy to the combustion is calculated by assuming diesel chemical formula to be C<sub>10.8</sub>H<sub>18.7</sub> with a lower heating value (LHV) of stoichiometric combustion of  $6.4 \times 10^6$  kJ/kmol [20].

Fig. 9 provides the calculated results of intake energy. With hydrogen flow rate of 22 and 220 SLPM, the energy added to the combustion is negligible for loads greater than 25%. However, at idle, the energy added from hydrogen increased by 6% and 93% for 22 and 220 SLPM respectively. This could be

a reasonable explanation for the observed reduction of CO<sub>2</sub> emissions since H<sub>2</sub> combustion does not emit CO<sub>2</sub>. As we noticed, CO<sub>2</sub> emissions reduced by 37% as energy added increased by 93%.

#### Increase in energy consumption due to electrolysis producing hydrogen

Gutierrez-Martin et al. [33] discussed the electrolysis process and the energy consumption of a typical process. A typical electrolysis process consumes:

$$W_u \approx 46 \left[ \text{kWh} / \text{kg}_{\text{H}_2} \right] \quad (7)$$

for the reaction of water decomposition at low temperatures, with a standard efficiency of conventional electrolysis at low current densities:  $\eta = 70\%$ . For a commercial product, such as HES 210, at a practical current density of about 2 A/cm<sup>2</sup> the cell voltage is about 2 V, the efficiency would be 74%, computed according to Gutierrez-Martin's method.

Using equation (7) and hydrogen density ( $8.38 \times 10^{-5}$  kg/l), power consumptions of the water electrolyzer at H<sub>2</sub> flow rates of 22 and 220 SLPM were estimated to be 5.1 kW and 51 kW respectively. It needs to be noted that the efficiency of electricity generation from engine mechanical power is assumed to be 100%. Based on the linear curves of mass based fuel consumption, according to engine power loads under varying hydrogen flow rates, with the hydrogen flow rate of 22 SLPM, a 5.1 kW of power load will increase the mass based fuel consumption by 1.75 kg/h. With the hydrogen flow rate of 220 SLPM, the potential increase in fuel consumption is 11.7 kg/h. The percentage of potential increased fuel consumption in measured fuel consumption for engine loads ranged from 75% to idle is listed in Table 5. For example, at 75% engine load, hydrogen production of 22 SLPM will increase fuel consumption by 2.6%, and hydrogen production of 220 SLPM will increase fuel consumption by 17.7%. The increased fuel consumption will also increase CO<sub>2</sub> specific emissions. The net effect of hydrogen injection on CO<sub>2</sub> specific emissions is listed in Table 5. For commercial H<sub>2</sub> flow rates, change in CO<sub>2</sub> specific emissions are within 5%.

#### Effect of hydrogen on operation at idle

Figs. 10 and 11 show results of continuous monitoring of engine power and speed during idle testing. It is obvious that engine stability is improved with hydrogen injection. One of

Table 5 – Percentage of increase of mass based fuel consumptions (kg/h) due to the increased electrical load of electrolysis for each engine load.

Engine load	Commercial value (22 SLPM)		High level (220 SLPM)	
	Net effect on CO <sub>2</sub> emission factors [%]	Increased fuel consumption [%]	Net effect on CO <sub>2</sub> emission factors [%]	Increased fuel consumption [%]
75%	3.8	2.6	18.1	17.7
50%	-4.6 <sup>a</sup>	3.9	11.7	27.1
25%	3.0	8.0	45.3	53.8
Idle	0.6	39.8	163.0	339.4

<sup>a</sup> A negative value indicates a decrease of CO<sub>2</sub> emission factors.

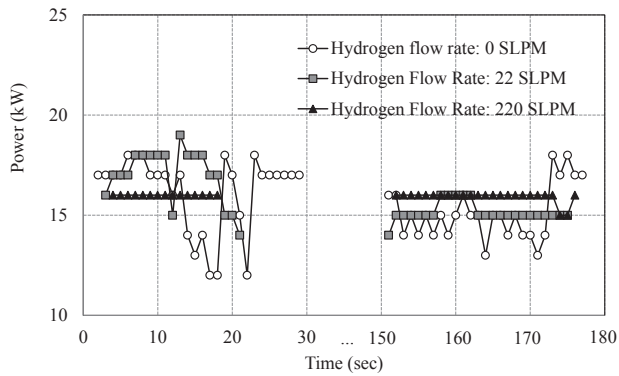


**Fig. 10 – Continuous monitoring of power during idle modes with hydrogen flow rates of 0, 22, and 220 SLPM.**

the main reasons for the stability enhancement under idle condition is that hydrogen contributes more to the output power, in contrast to higher load conditions. Due to the fast flame burning velocity of hydrogen, hydrogen oxidation occurs with less heat transfer to the ambient. In addition, the quenching gap of hydrogen is almost three times smaller than regular hydrocarbon fuel, which means that hydrogen flame can travel closer to the wall which results in a more complete combustion of the fuel. These combustion properties of hydrogen, as well as the ease of injection compared to diesel, are the main reasons for the more stabilized engine performance when hydrogen is injected into the intake manifold. Since during idle condition, higher percentage of output power is provided by the hydrogen, these effects are more prominent as compared to the higher load condition where most of the energy is provided by diesel rather than hydrogen.

## Summary and conclusions

The effect of adding hydrogen to a two-stroke marine diesel engine burning CARB ultra-low sulfur #2 diesel fuel was investigated by measurement following standard protocols. A DDC 12V-71Ti, 2-stroke marine engine was tested on an

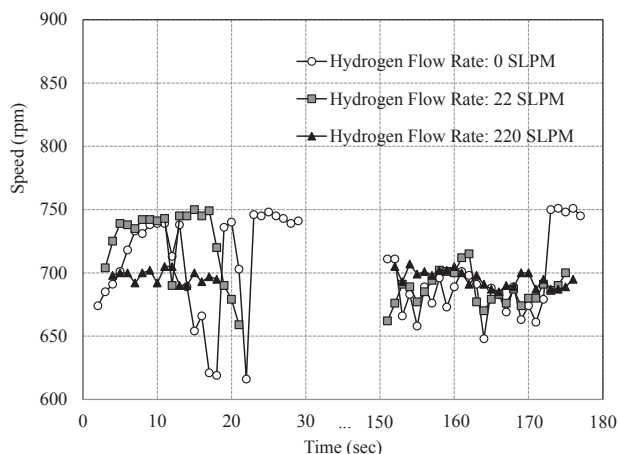


**Fig. 11 – Continuous monitoring of speed during idle modes with hydrogen flow rates of 0, 22 and 220 SLPM.**

engine dynamometer at idle and three loads specified in the ISO-8178 E3 protocol, with hydrogen flow rates of 0, 22 and 220 SLPM. Results showed hydrogen addition of 22 and 220 SLPM at idle reduced  $EF_{CO_2}$  by 21% and 37% respectively. The reductions of  $EF_{NO_x}$  were 28% and 41%, respectively; however, the  $EF_{PM_{2.5}}$  was increased by 40% and 85%, respectively.

With  $H_2$  flow rates of 22 SLPM and 220 SLPM, the reductions of overall  $EF_{CO_2}$  were 0.26% and 1.66%;  $EF_{NO_x}$  increased by 0.6% and reduced by 3.6% and  $EF_{PM_{2.5}}$  were reduced by 11% for both hydrogen flow rates. As is evident in this study, significant emission changes only occur when hydrogen contributes significantly to the total fuel energy.

Carbon dioxide emissions (kg/h) are directly proportional to the energy supplied by the diesel fuel. For greater than 20% engine load, calculations indicated that diesel fuel is the primary energy source. Results showed no benefit of adding hydrogen fuel up to 220 SLPM. At idle, energy release occurs from combustion of both diesel fuel and hydrogen, hence,  $EF_{CO}$  was reduced by 20.7% at 22 SLPM  $H_2$  injection and 37.3% at 220 SLPM  $H_2$  injection, corresponding to the energy added by hydrogen. The actual energy reduction for an engine with an electrolysis unit would be lower due to the energy requirements by the unit. Overall our study shows no significant benefit on the weighted  $EF_{CO_2}$ ,  $EF_{NO_x}$  and  $EF_{PM_{2.5}}$  of a marine diesel engine by adding hydrogen at up to 220 SLPM.

Although this paper provides a thorough insight into the impact of hydrogen injection on both criteria emissions as well as the fuel economy of compression ignition engines, more data are needed to support the finding from this study. As part of future work, we suggest to measure the engine in-cylinder pressure and temperature as well as the heat release rate in order to better understand the impact of hydrogen injection on the emissions from diesel combustion.

## Acknowledgments

The authors express their gratitude to the California Air Resources Board (CARB) for their financial support (Contract #08-421) and an anonymous company for offering their marine diesel engine to carry out this project successfully. An appreciation is extended to all the members for their support and cooperative efforts during the emission testing. The authors are grateful to Mr. Charles Buffalino and Mr. Kurt Bumiller for their assistance with the test preparations, Mr. Christian Bartolome and Mr. Arthur Peron for help with the testing and data collection, Ms. Xin Fan and Mr. James Gutierrez for providing analytical support, and Dr. Amin Akbari for helpful comments on the paper.

## REFERENCES

- [1] Verhelst S, Wallner T. Hydrogen-fueled internal combustion engines. *Prog Energy Combust Sci* 2009;35:490–527.
- [2] Rakopoulos CD, Scott MA, Kyritsis DC, Giakoumis EG. Availability analysis of hydrogen/natural gas blends combustion in internal combustion engines. *Energy* 2008;33:248–55.

- [3] Rao BH, Shrivastava KN, Bhakta HN. Hydrogen for dual fuel engine operation. *Int J Hydrogen Energy* 1983;8:381–4.
- [4] Li H, Karim GA. Knock in spark ignition engines. *Int J Hydrogen Energy* 2004;29:859–64.
- [5] Lee JT, Kim YY, Lee CW, Caton JA. An investigation of a cause of backfire and its control due to crevice volumes in a hydrogen fueled engine. *Trans ASME* 2001;123:204–10.
- [6] Varde KS, Frame GA. Hydrogen aspiration in a direct injection type diesel engine-its effects on smoke and other engine performance parameters. *Int J Hydrogen Energy* 1983;8(7):549–55.
- [7] Bika AS, Franklin LM, Kittelson DB. Emission effects of hydrogen as a supplement fuel with diesel and bio-diesel. SAE Paper; 2008. 2008-01-0648.
- [8] Kumar MS, Ramesh A, Nagalingam B. Use of hydrogen to enhance the performance of a vegetable oil fuelled compression ignition engine. *Int J Hydrogen Energy* 2003;28:1143–54.
- [9] Tsolakis A, Hernandez JJ, Megaritis A, Crampton M. Dual fuel diesel engine operation using H<sub>2</sub>. Effect on particulate emissions. *Energy Fuels* 2005;19:418–25.
- [10] Tomita E, Kawahara N, Piao Z, Fujita S, Hamamoto Y. Hydrogen combustion and exhaust emissions ignited with diesel oil in a dual fuel engine. SAE Paper; 2001. 2001-01-3503.
- [11] McWilliam L, Megaritis T, Zhao H. Experimental investigation of the effects of combined hydrogen and diesel combustion on the emissions of a HSDI diesel engine. SAE Paper; 2008. 2008-01-0156.
- [12] Shirk MG, McGuire TP, Neal GL, Haworth DC. Investigation of a hydrogen-assisted combustion system for a light-duty diesel vehicle. *Int J Hydrogen Energy* 2008;33:7237–44.
- [13] Pan H, Princevac M, Mahalingam S, Miller W, Khan Y, Jayaram V, et al. Effect of hydrogen injection on emissions from a marine diesel engine. Report to California Air Resources Board; 2011. Contrac #08–421.
- [14] Bari S, Esmail MM. Effect of H<sub>2</sub>/O<sub>2</sub> addition in increasing the thermal efficiency of a diesel engine. *Fuel* 2010;89:378–83.
- [15] Corbett JJ, Fischbeck PS. Emissions from ships. *Science* 1997;278(5339):823–4.
- [16] ISO. ISO 8178–4. Reciprocating internal combustion engines-exhaust emission measurement. Part-4: test cycles for different engine applications; 1996.
- [17] ISO. ISO 8178–1. Reciprocating internal combustion engines – exhaust emission measurement – part 1: test-bed measurement of gaseous and particulate exhaust emissions.
- [18] Beardsley M, Lindhjem CE. Exhaust emission factors for non road engine modeling – compression ignition. Report no.: NR-009. US EPA, Office of Mobile Sources, Assessment and Modelling Division; 1998 February 24.
- [19] Russel RL, Yusuf Khan M, Welch WA. On-board ISO 8178–4 D2 marine engine measurement of emission from caterpillar generator engine using ULSD and a 50/50 blend of ULSD and algal based biofuel [http://www.marad.dot.gov/documents/MARAD\\_ALT\\_FUEL\\_REPORT\\_APPENDIX\\_F.pdf](http://www.marad.dot.gov/documents/MARAD_ALT_FUEL_REPORT_APPENDIX_F.pdf); 2012.
- [20] College of the Desert. Hydrogen use in internal combustion engines <http://www1.eere.energy.gov>; 2001.
- [21] Heywood JB. *Internal combustion engine fundamentals*. McGraw-Hill; 1988.
- [22] Frassoldati A, Faravelli T, Ranzi E. A wide range modeling study of NO<sub>x</sub> formation and nitrogen chemistry in hydrogen combustion. *Int J Hydrogen Energy* 2006;31:2310–28.
- [23] Fenimore CP. Formation of nitric oxide in premixed hydrocarbon flames. In: 13th symp. (int'l.) on combustion. The Combustion Institute; 1971. p. 373.
- [24] Kerley RV, Thurston KW. The indicated performance of Otto-cycle engine. SAE Trans 1962;70:5–30.
- [25] Rortveit G, Hustad JE, Li SC, Williams FA. Effects of diluents on NO<sub>x</sub> formation in hydrogen counterflow flames. *Combust Flame* 2002;130:48–61.
- [26] Dec J, Canaan R. PLIF imaging of NO formation in a DI diesel engine1. SAE Technical Paper; 1998. 980147.
- [27] White CM, Steeper RR, Lutz AE. The hydrogen-fueled internal combustion engine: a technical review. *Int J Hydrogen Energy* 2006;31:1292–305.
- [28] Moreno F, Muñoz M, Magén O, Monne C, Arroyo J. Modifications of a spark ignition engine to operate with hydrogen and methane blends. In: International conference on renewable energies and power quality, Granada (Spain), 23th to 25th March, 2010.
- [29] Turns SR. *An introduction to combustion: concepts and applications*. 2nd ed. New York: McGraw-Hill; 2000.
- [30] Li H, Shade B, Clark N, Thompson G, Wayne S, Gautam M. An experimental evaluation of NO<sub>x</sub> reductions from H<sub>2</sub> enhanced diesel combustion. Review Report; 2009.
- [31] Gatts T, Li H, Liew C, Liu S, Spencer T, Wayne S, et al. An experimental investigation of H<sub>2</sub> emissions of a 2004 heavy-duty diesel engine supplemented with H<sub>2</sub>. *Int J Hydrogen Energy* 2010;35(20):11349–56.
- [32] Kingham S, Durand M, Aberkane D, Harrison J, Wilson JG, Epton M. Winter comparison of TEOM, MiniVol and DustTrak PM<sub>10</sub> monitors in a woodsmoke environment. *Atmos Environ* 2006;40:338–47.
- [33] Gutierrez-Martin F, Garcia-De Maria JM, Bairi A, Laraqi N. Management strategies for surplus electricity loads using electrolytic hydrogen. *Int J Hydrogen Energy* 2009;34:8468–75.